Phys. Status Solidi C **7**, No. 7–8, 2259–2261 (2010) / **DOI** 10.1002/pssc.200983541

physica status solidi c
www.pss-c.com
current topics in solid state physics

Simulations of laser diodes with nonpolar InGaN multi-quantum-wells

Z. Q. Li[*,1], Z. M. Simon Li[1], and Joachim Piprek[2]

[1] Crosslight Software Inc., 121-3989 Henning Drive, Burnaby, BC V5P 6P8, Canada
[2] NUSOD Institute LLC, P.O. Box 7204, Newark, DE 19714-7204, USA

Received 30 September 2009, revised 2 February 2010, accepted 4 February 2010
Published online 12 May 2010

Keywords InGaN, quantum wells, laser, simulations

[*] Corresponding author: e-mail zqli@crosslight.com, Phone: +1-604-320-1704, Fax: +1+604-320-1734

Simulations of the characteristics of laser diodes (LD) with non-polar and InGaN multi-quantum-wells (MQW) have been conducted in multi-dimensional drift-diffusion model. The strain coefficients of the QWs of arbitrary crystal-orientations are obtained by minimizing the total strain energy. Electronic structure and optical gain of non-polar InGaN QWs are calculated by the 6x6 k.p theory. Finally by integrating the gain and effective mass models of non-polar InGaN QW into our LASTIP software package, we simulated the performance of the laser diodes with non-polar MQWs, and the results are compared with the experiments.

1 Introduction

Quantum wells (QWs) based on gallium nitride and related materials are of great interest for the applications in laser diodes (LD) and light-emitting diodes (LEDs) with wavelength range from ultra-violet to green [1]. The c-plane (0001) wurtzite GaN QWs suffer from high strain-induced piezoelectric (PZ) and spontaneous (SP) polarization [2], which generate build-in electric fields along the (0001) direction. The polarization field causes a spatial separation of electron and hole wavefunctions resulting in a lower recombination efficiency, reduced oscillator strength, and redshifted emission. To overcome the deficiencies of c-plane GaN QWs, non-polar and semi-polar QWs have been investigated for higher efficiency and stronger light power output from the devices [3,4]. Park and Chuang [5] have studied theoretically the effects of crystal-orientation on the electronic and optical properties of strained InGaN QWs. They found that the effective masses and optical matrix elements show strong anisotropy in the QW plane, and the optical gain of y-polarization is much larger than that of x-polarization.

Although, there have been extensive theoretical investigations on the band structure, optical dipole momentum matrix and optical gain of non-polar InGaN QWs [6], there is no theoretical investigation regarding the effects of crystal orientation on the performance of laser diodes, to our best knowledge. In this paper, we extended previous theoretical studies of non-polar GaN QWs, and integrated the relevant models into our in-house LASTIP software package, which enables us to study the effects of crystal orientation on the characteristics of a typical InGaN-based QW laser.

2 Theoretical models

We begin with the calculations of strain coefficients at arbitrary growth orientation. Here we assume that the substrate is unstrained, and the epi-layer is pseudomorphically grown on the substrate. Thus the strain tensor ε_{ij} can be obtained by minimizing the strain energy density given by

$$W = \frac{1}{2}\sum_{i,j}\int C_{ij}\varepsilon_i\varepsilon_j dV \qquad (1)$$

under the condition of commensurability between substrate and epi-layer. Analytical solutions have been given for some special cases, but for arbitrary growth orientations, numerical calculations have to be performed. The Hamiltonian for an arbitrary crystal orientation can be obtained using a rotation matrix

$$U = \begin{pmatrix} cos\theta cos\psi & cos\theta sin\psi & -sin\theta \\ -sin\phi & cos\psi & 0 \\ sin\theta cos\psi & sin\theta sin\psi & cos\theta \end{pmatrix} \quad (2)$$

Rotation of the Euler angles θ and ψ transform the physical quantities from (x, y, z) coordinates to (x', y', z') co-ordinates. The z axis is the c-axis [0001], and the growth axis z' is normal to the QW plane. The relation between the coordinate systems for the vectors and the strain tensors is given as

$$k_i' = U_{i\alpha} k_\alpha \quad (3)$$

$$\varepsilon_{ij}' = U_{i\alpha} U_{j\beta} \varepsilon_{\alpha\beta}$$

where summation over repeated indices is implied. Using Eq. (1)-Eq. (3), the Hamiltonian for an arbitrary crystal orientation $H(k', \varepsilon')$ can be obtained from the Hamiltonian of [0001] orientation $H(k, \varepsilon)$ given in [5]. The electronic structure, optical dipole momentum matrix and optical gain of InGaN QW are thus calculated based on the Hamiltonian.

3 Results

3.1 Optical gain calculation

The calculated results of an $In_{0.15}Ga_{0.85}N$/GaN 3-nm QW are given in this section and all material parameters are from Ref. [5]. The QW is grown on an m-plane substrate ($\theta = 90^\circ, \psi = 90^\circ$) for the purpose of calibration. However, the program can handle arbitrary growth orientation.

Figure 1 shows the band dispersions of top 3 valence bands along in-plane k_x and k_y directions.

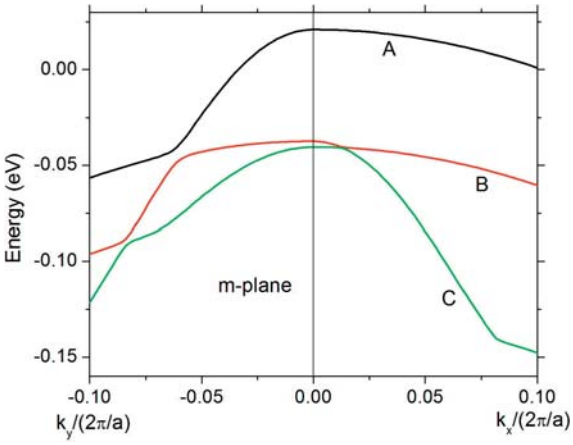

Figure 1 Band structure of m-plane InGaN/GaN QW. A,B and C indicate the top three valence band.

Unlike the c-plane QW, the band structure of m-plane QW shows that the hole effective mass of the top A band is smaller in k_y direction than in k_x direction. The anisotropy of band structure also results in the difference of optical matrix elements for different polarizations. In Fig. 2 and Fig. 3, we depict the optical matrix elements of m-plane InGaN/GaN QW with polarization along x and y directions, respectively. We see again the y-polarization optical matrix elements are higher for the A band near $k = 0$, which is more relevant to the optical gain.

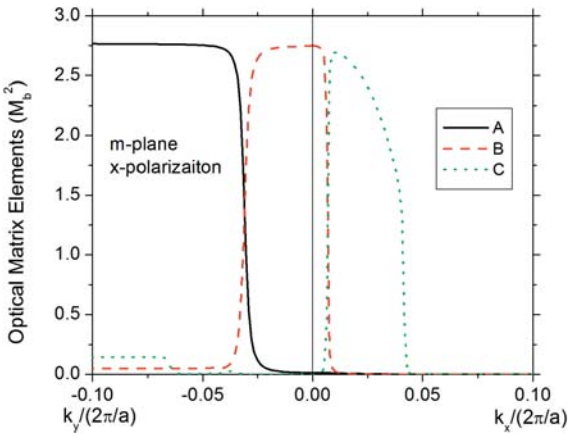

Figure 2 Optical matrix elements of m-plane InGaN/GaN QW for x-polarization. A,B and C indicate the top three valence band.

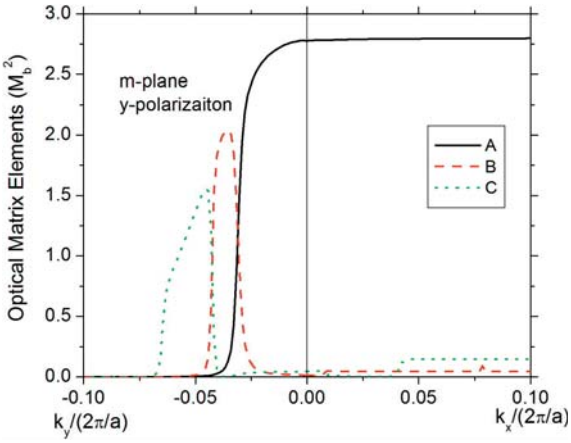

Figure 3 Optical matrix elements of m-plane InGaN/GaN QW for y-polarization. A,B and C indicate the top three valence band

The optical gain is calculated using the following equation

$$g(\omega) = \sum_{m,n} \sqrt{\frac{\mu_0}{\varepsilon}} \left(\frac{e^2}{m_0^2 \omega}\right) \int_0^{2\pi} d\psi \int_0^{\infty} dk_{\|} \quad (4)$$

$$\times \frac{2k_{\|}}{(2\pi)^2 d} |M_{nm}|^2 (f_v^m - f_c^n) L(\omega)$$

where d is the thickness of the QW, and $|M_{nm}|^2$ is the optical momentum matrix elements, and other notations have common meaning. $L(\omega)$ is Lorentzian shape function.

The results of optical gain for c-plane (piezo-charge and spontaneous charge are not included) and m-plane are given in Fig. 4. For m-plane QW, the y-polarization optical gain is substantially enhanced compared with the c-plane

QW, although the polarization charge is omitted in the calculations.

The optical gain and effective mass of InGaN QWs on arbitrary crystal orientations have been integrated into the LASTIP software [7] for the laser simulations, and are easily accessed through the friendly graphic user interface.

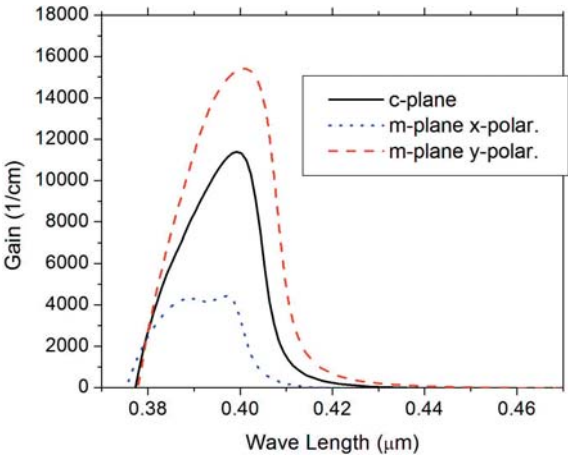

Figure 4 Optical gain spectra of c-plane and m-plane InGaN/GaN QWs.

3.2 Laser simulation

As a practical example, we simulate the 5-QW m-plane laser structure described in [8]. The $In_{0.12}Ga_{0.88}N$/GaN quantum wells are 8nm thick and provide sufficient waveguiding so that cladding layers are not present in this device. However, a 10 nm thick $Al_{0.2}Ga_{0.8}N$ layer is included to reduce electron leakage into the p-doped layers.

Our isothermal multi-mode simulation of pulsed laser operation assumes common numbers for the material parameters [9]. The QW Shockley-Read-Hall recombination lifetime and the optical loss are the only fit parameters to find agreement with the measured light-current curve (Fig. 5). While the fitted lifetime of 1.5 ns lies within the expected range, the optical loss of 140/cm is rather large and it is partially attributed to strong photon scattering at the etched facets. Electron leakage current into the p-layers is found to be negligible, due to the large conduction band offset of the AlGaN stopper layer. The simulated energy band diagram is shown in Fig. 6. It reveals some potential drop in the undoped MQW barriers which contributes to the overall device bias.

In summary, we have successfully integrated the effective mass and optical gain models of non-polar InGaN QWs into the LASTIP software package, which is a multi-dimensional finite-element simulator of semiconductor devices. With this powerful tool, for the first time we can study the effects of crystal orientations on the performance of laser diodes based on non-polar InGaN-QWs.

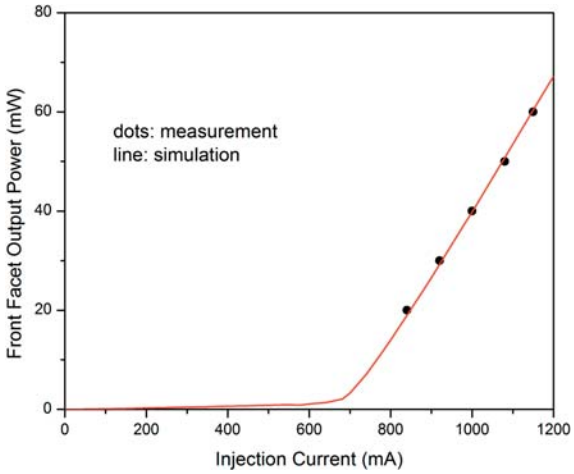

Figure 5 Comparison of light-current characteristics. Experimental results are from Ref. [7].

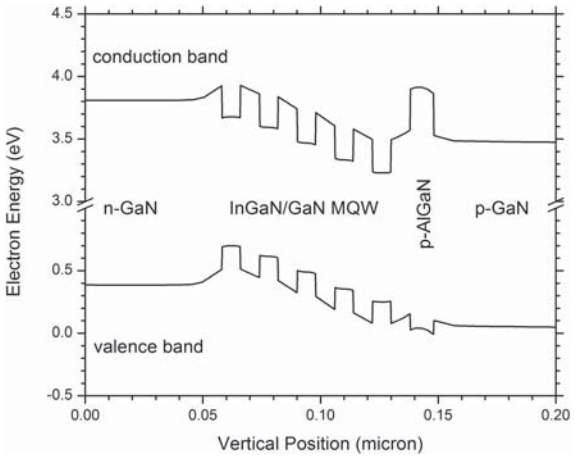

Figure 6 Simulated energy band diagram above lasing threshold.

References

[1] S. Nakamura and F. Fasol, The Blue Laser Diodes (Springer-Verlag, Berlin, 1997).
[2] F. Bernardini, V. Fiorentini, and D. Vanderbilt, Phys. Rev. B **56**, 10024 (1997).
[3] P. Waltereit, O. Braudt, A. Trampert, H.T. Grahn, J. Menniger, M. Ramsteriner, M. Reiche, and K.H. Ploog, Nature **206**, 865 (2000).
[4] Y.J. Sun, O. Brandt, S. Cronenberg, S. Dhar, H.T. Frahn, K.H. Ploog, P. Waltereit, and J.S. Speck, Phys. Rev. B. **67**, 041306 (2003).
[5] S.H. Park and S. L. Chuang, Phys. Rev. B **56**, 4725 (1999).
[6] M. V. Kisin et. al., J. Appl. Phys. **105**, 013112 (2009), and references therein.
[7] Lastip User's Manual, 2008, Crosslight Software Inc., www.crosslight.com
[8] D.F. Feezell, M.C. Schmidt, R.M. Farrell, K.C. Kim, M. Saito, K. Fujito, D.A. Cohen, J.S. Speck, S.P. DenBaars, and S. Nakamura, Jpn. J. Appl. Phys. **46**, L284 (2007).
[9] J. Piprek (ed.), Nitride Semiconductor Devices - Principles and Simulation (Wiley-VCH, Weinheim, 2007).